MADELUNG ENERGIES AND SITE PREFERENCES IN AMPHIBOLES. I

E. J. W. WHITTAKER, *Department of Geology and Mineralogy, Parks Road, Oxford, England.*

ABSTRACT

Madelung energies and electrostatic potentials at all ionic sites have been computed for a total of about 120 different ionic arrangements corresponding to 14 clinoamphibole species, each in hydroxy and fluoro forms. The calculations have been repeated on the basis of the atomic co-ordinates in both the cummingtonite and glaucophane structures. It is shown that the results agree qualitatively and semi-quantitatively with the known preference of Y^{3+} ions for $M(2)$ sites in glaucophane, riebeckite and magnesio-riebeckite and of Z^{3+} ions for $T(1)$ sites in pargasite. On the basis of the results seven types of site preference are predicted which have not yet been observed in clinoamphibole structures.

INTRODUCTION

It is now well known as a result of X-ray structure analyses of magnesio-riebeckite (Whittaker, 1949) and glaucophane (Papike and Clark, 1969) that in alkali amphiboles the trivalent ion (Fe^{3+} or Al) preferentially occupies the $M(2)$ site. This was explained by Whittaker (1949) as arising from the lower electrostatic potential at $M(2)$ that results from its proximity to the $M(4)$ site, which is occupied by the sodium ion. Such an explanation is still believed to be true in essence, but as originally put forward it begs a number of questions, and is to a considerable extent based on the common, but unsubstantiated, supposition that tremolite examplifies the most normal amphibole structure. If this is assumed, then in deriving glaucophane from tremolite one can argue that Na replaces Ca in $M(4)$ because it is too large to enter the other sites. The balancing substitution of Al for Mg then goes into $M(2)$ in order to keep the overall charge distribution as similar as possible to that in tremolite. However, it is by no means self-evident that the charge distribution in tremolite (*i.e.* 2+ in each site $M(1)$, $M(2)$, $M(3)$, and $M(4)$) is the most stable one. In tremolite, and in various other amphiboles where only divalent ions are present, it is necessarily imposed by the composition, but in those amphiboles where this constraint is lifted it is quite possible that the pattern of charge distribution that is manifested will be a fundamentally more stable one, rather than merely a second best approximation to that in tremolite. Such a possibility is rather suggested by the structure of holmquistite (Whittaker, 1969), in which Li is segregated in $M(4)$ and Al in $M(2)$. Unlike the case of Na in alkali amphiboles there is no size consideration to constrain Li to occupy $M(4)$. One has therefore no firm datum from which to begin the argument regarding the proximity of Al to Li. One must probably argue that the optimum charge distribution is one

with a lower charge than 2 at $M(4)$, and that once this is established then once again Al will go to $M(2)$: but at least a contributory cause of the observed ionic distribution could be that the optimum charge distribution is one with a higher charge than 2 at $M(2)$, regardless of the charge at $M(4)$.

In simpler structures the preferences of different sites for ions of different charges can be derived on the basis of Pauling's electrostatic valency rules. These are difficult to apply unambiguously to the amphibole structure because of uncertainty about the co-ordination number of $M(4)$. The ion at this site makes short bonds to four nonbridging oxygens (two $O(2)$ and two $O(4)$) but its distances from other oxygens are intermediate between obviously bonded and obviously non-bonded values. Moreover these other oxygens are bridging oxygens already bonded to two silicon atoms. Donnay and Allman (1970) have devised a relationship between electrostatic bond strength and bond length on the basis of which $M(4)$ has to be regarded as only IV co-ordinated in some amphiboles (notably grunerite). But even on such a basis one cannot obtain a quantitative estimate of the preference energy of ions of different charges for different sites. The same may be said of the considerations of electrostatic bond strength and shielding factors which Gait and Ferguson (1970) have applied to the tendencies to segregation of Si and Al in feldspars.

In addition to the segregation of mono- and tri-valent ions in amphiboles there have been a number of studies of the question of the segregation of Fe^{2+} and Mg, both by X-ray diffraction (Zussman, 1955; Ghose, 1961) and by a combination of infra-red and Mössbauer spectroscopy (Bancroft and Burns, 1969). The effects observed are now usually interpreted in terms of differences in crystal field stabilisation energy of Fe in the different sites, arising from different distortions from ideal octahedral symmetry, although different tendencies to covalent bond formation in different sites had earlier been invoked by Ghose (1961). Because of the different degrees of ionicity in their bonding, Mg and Fe must however bear different real charges as distinct from nominal charges. Their distribution is therefore likely to be affected not only by crystal field effects but also by the optimum pattern of charge distribution in the different sites.

Studies of the distribution of tetrahedral Al in amphiboles have only been made recently (Papike, Ross, and Clark, 1969). Such distributions will clearly be affected in similar ways by the optimum pattern of charge distribution. Furthermore they may well affect, and be affected by, the charge distribution in the M sites.

A knowledge of the mechanism of site preferences is relevant not only to an understanding of the detailed structure of specific amphiboles, but

also to a prediction of the relative accessibility of the different sites to elements present only in trace quantities, which is a significant geo-chemical problem.

Relative Energies of Different Ion Distributions

The original suggestion regarding the preference of a trivalent ion for $M2$ in an alkali amphibole (Whittaker, 1949) was in terms of the relative electrostatic potentials at different sites. With present day computing facilities it is possible to calculate such differences, but further considera-tion shows that it is not sufficient merely to calculate the potentials at the M sites: when these sites are filled in any particular way this will react on the potentials at the O and Si sites and thus modify the energy of the whole structure. What must be compared are therefore the Madelung energies for the structures that would arise from filling the M sites (and the tetrahedral sites) in a variety of ways. Because of the close geometrical similarity of all such structures the short-range repul-sion terms will be, to a first approximation, independent of the details of the ionic distribution, and the site preference energies for ions of dif-ferent charges will therefore be given by the differences in Madelung energies of appropriate ion distributions.

However, except in unusual circumstances it is found that site pref-erences in charge balancing substitution can in fact be predicted qualita-tively from the electrostatic potentials at the cation sites in the structure that is regarded as the parent one in the substitution. A knowledge of these individuals potentials is therefore very valuable, and in all cases the Madelung energy

$$U = \sum_i q_i V_i$$

(where ionic charges are q_i and the summation is over all the ions in one unit cell) has been computed in two stages, and the values of the site potentials V_i have been accumulated separately and recorded for use in this way.

Computation of Madelung Energy: Principles

Boeyens and Gafner (1969) have discussed the advantages of direct summation of the Madelung function rather than the use of the more complicated mathematical functions and corrections that were necessary before such direct summation was practicable. The advantages are even greater in a complicated structure like an amphibole as compared with the simpler structures discussed by Boeyens and Gafner.

Computation was carried out for the clino-amphiboles entirely on the basis of a primi-tive unit cell centered on the $M(3)$ site and having its vertices at $(\pm a/2, 0, \pm c/2)$ and $(0, \pm b/2, \pm c/2)$ in terms of the usual co-ordinates based on the C-centered cell. This is
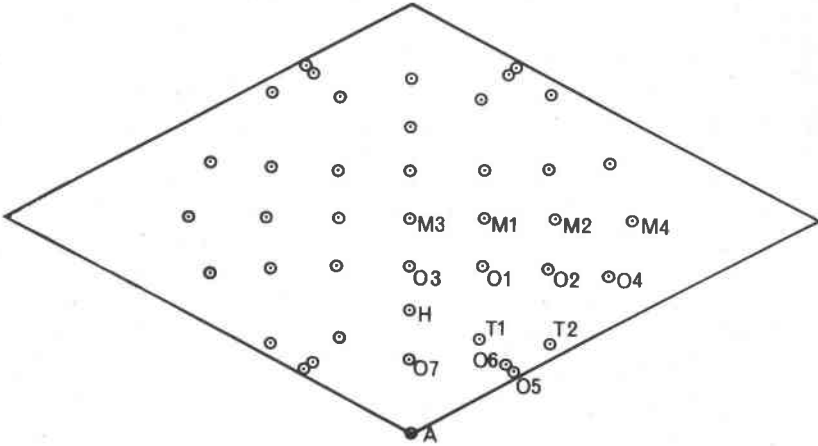
FIG. 1. The primitive cell of clino-amphibole projected on (001).

shown in projection on (001) in Figure 1. This cell was surrounded by successive shells of cells, the rth shell having its vertices at $(\pm a(r+\frac{1}{2}), 0, \pm c(2r+\frac{1}{2}))$ and $(0, \pm b(r+\frac{1}{2}), \pm c(2r+\frac{1}{2}))$. The computed energy therefore converged to the Madelung energy of a crystal bounded by the forms {110} and {001} and having edge-lengths in the ratio $1:1:4c/(a^2+b^2)^{1/2}$. The shells were made two unit cells thick in the c-direction to make the shape as equidimensional as possible. This avoids uneconomic computing to unnecessarily great distances in the a- and b-directions while the limits in the c-direction are being extended sufficiently far to make the summation converge. With this arrangement adequate convergence was obtained by inclusion of the 3rd shell; that is the summation extended to a minimum radial distance of rather over 30 Å from the center along the normals to the bounding planes.

It was observed that the convergence of the summation for the potential at an atomic site was in general slower the further removed that site was from the center of the cell at the $M(3)$ site. This occurs because the minimum radial distance to which the summation extends from such an eccentric site is appreciably less than for a central site, the relative difference in this distance being up to 33 percent in the first shell, and up to 14 percent even in the third shell. In order to eliminate this difference the possibility was considered of shifting the origin of the primitive unit cell to each atomic site in turn. However, a much more serious problem then arises. The outer boundaries of the outermost shell used in computing the potential at the ith site are displaced from those used in computing the potential at any other site, e.g. the central site $M(3)$. In Figure 2 the ith site is shown for the sake of simplicity in a direction from $M(3)$ parallel to an edge of the cell. The new boundary of the outermost shell is thus $A'B'C'D'$ instead of $ABCD$. Given that the structure is centrosymmetric about $M(3)$, the contents of $CC'D'D$ (now "vacated") are identical to those of $ABC''D''$ as well as $AA'B'B$. The change from $ABCD$ to $A'B'C'D'$ is therefore the same as that obtained by subtracting the contents of $ABD''C''$ and adding the contents of $ABB'A'$. It is therefore equivalent to adding a sheet of dipoles on the face AB, and this will modify the potential V_i by a finite amount which will be independent of the size of the outermost shell. Potentials calculated in this way would therefore not be comparable with one another, except after making very complicated corrections. It is therefore better to accept the slower convergence for eccentric sites and retain constant cell and shell boundaries throughout.
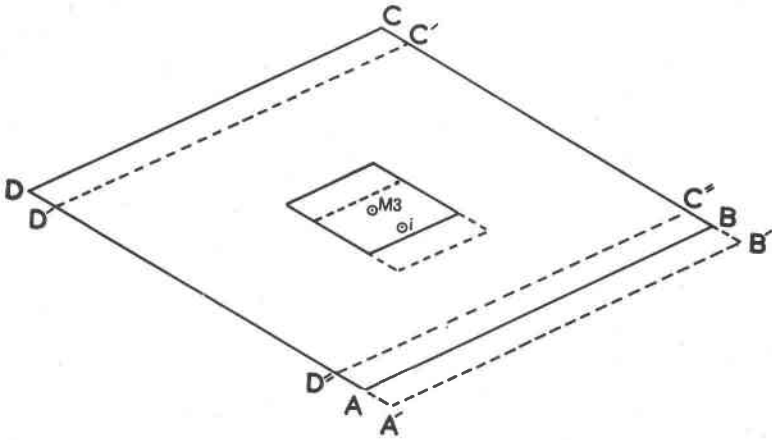
FIG. 2. The full lines show the central cell and the boundary of the 3rd shell ($ABCD$) when the cell is centered at $M3$. When the centre of the cell is shifted to the ith atom, the boundary of the 3rd shell is shifted to $A'B'C'D'$. There is a resulting dipolar sheet on the face AB equivalent to adding all the charges in $AB'B'A'$ and subtracting the (same) charges that occur in $ABC''D''$.

The distribution of atomic sites in an infinite clinoamphibole crystal is centro-symmetric about $M(3)$, but ions at the $M(1)$ and $M(4)$ sites lie on the surface of the primitive cell, and when the A-site is occupied this ionic site lies on an edge of the primitive cell. The cell therefore has a dipole unless an Evjen cell (Evjen, 1931) is adopted. The use of such a cell requires the assignment of half the charge of surface ions to the equivalent sites on opposite surfaces of the cell, and of a quarter of the charge on edge ions to the four equivalent sites on four parallel edges. As shown by Boeyens and Gafner (1969) the same result can be obtained more economically by using the ordinary cell combined with an Evjen surface. The redistribution of charge is then carried out only on the surface of the outermost shell, and this procedure has been adopted here.

A further difficulty arises when ionic substitutions are considered that are not compatible with the centro-symmetry of the structure, and that therefore result in a structure with a permanent dipole. A straight forward computation correctly evaluates the potential distribution within a finite crystal possessing such a dipole, but this is not a relevant physical object. There appear to be three possibilities:

(i) the symmetry is reduced in this way, and the crystal adsorbs counter-ions of some kind at the surface to neutralise the dipole;

(ii) a domain structure is adopted, with a zero average dipole;

(iii) a disordered structure is formed in which the centro-symmetry is retained in a statistical sense.

The type of program used in the present investigation is not able to deal with (iii), which clearly requires further investigation, perhaps using the methods devised by Jagodzinski (1967). In (ii) the structure within a domain will be subject to the field due to the charge on the surfaces of the surrounding domains which neutralize its own dipole. In both (i) and (ii) therefore the effect is that of an oppositely directed dipolar surface surrounding

the crystal. This will modify the potential at all sites in the central unit cell, and it is necessary to calculate correction terms arising from this and to add these to the site potentials.

COMPUTATION OF MADELUNG ENERGY: TACTICS

The required computation can be symbolised as:

$$U = \sum_i q_i V_i \tag{1}$$

and

$$V_i = \sum_r \sum_{hkl} \sum_j q_j / d_{ij(rhkl)} \tag{2}$$

where:

q_i, q_j are the charges on the ith and jth ions;

$d_{ij(rhkl)}$ is the distance of the ith ion in the central cell from the jth ion in the cell h, k, l. The center of the cell h, k, l lies at $ha/2$, $kb/2$, lc. Strictly speaking the parameter r is unnecessary. It is introduced in order to follow the process of convergence by shells, and an appropriate relationship between h, k, and l is introduced in each shell.

The most time consuming part of the computation is the square root involved in calculating d_{ij}. In computing to three shells about 5×10^5 values of d_{ij} are required, and the total computing time was about 40 minutes on a KDF9 computer. Since a very large number of permutations of substituent ions are to be considered (several hundred) it was obviously necessary to avoid carrying out the whole computation for each one. Although the infinite sum for V_i only converges provided that the summation over j is performed first, once fixed limits have been set for the summations the order of summation is immaterial. Thus

$$V_i = \sum_j q_j C_{ij} \tag{3}$$

where

$$C_{ij} = \sum_r \sum_{hkl} 1/d_{ij(rhkl)} \tag{4}$$

Accordingly the results of the computation were accumulated in two forms: as total contributions from successive shells to check convergence: and as partial contributions C_{ij} from all the jth atoms in the whole region. The latter were output on paper tape and subsequently recombined via equations (3) and (1) with a great variety of q_i and q_j values. This required only short programs involving a computing time of less than 1 second per variant on an Atlas computer.

In order to calculate the effects of the Evjen surface and the other dipolar effects discussed in the preceding section, the following procedure was adopted.

The dipole moment of the primitive (non-Evjen) cell was considered to be resolved into components D_x, D_y, D_z, parallel to the x, y, and z axes. The charges required to neutralise the dipole were then considered to be situated at the centers of cell faces on the bounding forms $\{110\}$ and $\{001\}$ and the effects of these charges on the potentials at all sites in the cell at the origin were computed for unit values of D_x, D_y, and D_z. This computation was done once and for all, and the results were multiplied by the actual values of D_x, D_y, and D_z computed for each individual case. A subsidiary computation for the true Evjen surface required to compensate for the $M1$ and $M4$ ions on the cell surface showed that there was a

negligible error arising from lumping the charges at the centers of cell faces rather than putting them at their true co-ordinates on the cell faces.

RESULTS

General Observations on Site Potentials. The full computation was carried out twice, once using the cummingtonite structure (Ghose, 1961) and once using the glaucophane structure (Papike and Clark, 1969). Results were obtained for each of these by incorporating charges either of -2 and $+1$, or of -1 and 0, at the $O(3)$ and H sites respectively, in order to simulate hydroxy and fluoro species. A small number of oxy-amphibole variants was also investigated by using a charge of -2 at $O(3)$, zero at H, and a compensating increased charge at M sites.

The most generally indicative set of results for the potentials at individual ionic sites are those based on the cummingtonite structure, with all M sites assumed to be occupied by ions of charge $2+$. These are shown in columns 2 and 3 of Table 1, for the hydroxy- and fluoro-amphibole respectively. As would be expected, structurally similar sites have very similar potentials; in the fluoro case the ranges for similar sites are within the following limits

TABLE 1. SITE POTENTIALS (IN $e^2\text{Å}^{-1}$) IN A FEW CLINO-AMPHIBOLE ARRANGEMENTS

Site	All M sites M^{2+};		all T sites T^{4+}		$M(2)^{3+}M(4)^+$		$M(1)^{3+}M(2)^+$
	cummingtonite co-ords		glaucophane co-ords		cummingtonite co-ords		
	OH	F	OH	F	OH	F	OH
$M(3)$	-1.719	-1.439	-1.903	-1.625	-1.422	-1.143	-1.495
$M(1)$	-1.726	-1.476	-1.905	-1.657	-1.485	-1.233	-2.066
$M(2)$	-1.776	-1.700	-2.163	-2.087	-2.089	-2.013	-1.364
$M(4)$	-1.508	-1.474	-1.385	-1.359	-0.945	-0.911	-1.650
$T(1)$	-3.233	-3.236	-3.341	-3.338	-3.079	-3.079	-3.190
$T(2)$	-3.230	-3.217	-3.328	-3.314	-3.138	-3.125	-3.313
A	-0.246	-0.369	-0.313	-0.440	-0.126	-0.249	-0.206
H	-1.504	(-0.387)	(-1.657)	(-0.536)	(-1.306)	(-0.190)	-1.284
$O(3)$ [F]	$+1.877$	$+0.959$	$+1.707$	$+0.789$	$+2.118$	$+1.200$	$+2.270$
$O(7)$	$+2.204$	$+2.151$	$+2.129$	$+2.082$	$+2.351$	$+2.298$	$+2.280$
$O(1)$	$+1.920$	$+2.052$	$+1.726$	$+1.857$	$+2.237$	$+2.369$	$+2.029$
$O(2)$	$+1.917$	$+1.984$	$+1.769$	$+1.839$	$+2.085$	$+2.152$	$+1.853$
$O(4)$	$+1.900$	$+1.934$	$+1.817$	$+1.854$	$+1.983$	$+2.017$	$+1.658$
$O(5)$	$+2.189$	$+2.174$	$+2.127$	$+2.112$	$+2.298$	$+2.283$	$+2.131$
$O(6)$	$+2.213$	$+2.190$	$+2.182$	$+2.162$	$+2.269$	$+2.246$	$+2.215$

In the fluoro-amphiboles F occupies $O(3)$, and the potential at the position occupied by H in the hydroxy-amphiboles is given in parenthesis because it is not an actual atomic site.

$M(1)$, $M(3)$	0.037
$T(1)$, $T(2)$	0.019
$O(1)$, $O(2)$, $O(4)$	0.118
$O(5)$, $O(6)$, $O(7)$	0.039

(all in potential units of $e/\text{Å}$), and the ranges for the hydroxy case are much smaller still. In both cases $M(2)$ is the most negative of the M sites, by 0.050 in the hydroxy and by 0.224 in the fluoro case; and $T(1)$ is slightly the more negative of the T sites. The main difference between the two cases is that $M(1)$ and $M(3)$ are much less negative in the fluoro-compound relative to other sites, and as a result $M(3)$ becomes just the least negative M site in the fluoro compound, instead of $M(4)$ in the hydroxy-compound. The A site is always much less negative than any of the M sites.

On the basis of these results it would be expected that, other things being equal, $M(2)$ would be the preferred site for Y^{3+} ions, $T2$ for Z^{3+} ions and $M(4)$ for X^{1+} (or Y^{1+}) ions, except in fluoro-amphiboles where Y^{1+} might occupy $M(3)$ preferentially. The A site would always be discriminated against by ions of charge greater than unity. It will be seen below that there is a strong tendency towards these being the energetically preferred sites, although other factors can modify the results in some circumstances. Indeed, as soon as Y^{3+} and Y^{1+} ions are inserted in $M(2)$ and $M(4)$ sites the potential distribution is altered dramatically, as may be seen from Table 1, columns 6 and 7. This alteration is in a direction which stabilises the substitution that has been made. If the substitution is made in sites that would not be expected to be the preferred ones (Table 1 column 8) this self-stabilising effect is again observed and can more than off-set the original difference in potential between $M(1)$ and $M(4)$. This result shows the importance of using the total Madelung energy, rather than merely the potential distribution, in assessing the relative preferences of different sites for ions of differing charge when these are inserted systematically (*i.e.*, so as to change the species).

When the site potentials are calculated for a structure having its atoms at the co-ordinates of the glaucophane structure, but with equally charged $2+$ ions at all M-sites, the potentials are as shown in columns 4 and 5 of Table 1. Comparison with columns 2 and 3 shows that the potential at $M(2)$ is much lower and that at $M(4)$ much higher than in the case of cummingtonite. This is due to the small size of Al which occupies $M(2)$ in glaucophane (compared with Mg, Fe in cummingtonite) and the large size of Na at $M(4)$ in glaucophane (compared with Fe in cummingtonite); as a result of these size differences the nearest anionic neighbours are inevitably at different distances from these sites and have

a purely local effect on their potentials. This again reinforces the effect of putting Y^{3+} at $M(2)$ and X^{1+} at $M(4)$, but is not relevant to the preference of these ions for these sites, as it would occur wherever they were actually substituted.

Site Preferences from Madelung Energies. In order to obtain a quantitative measure of the preference energy for segregation of ions of particular charge in particular sites, the Madelung energies for a substantial number of different ionic distributions were calculated corresponding to each of the 13 integral points in amphibole charge distribution space (Whittaker, 1968) as shown in Table 2. Even this number of distributions is far from exhausting all the theoretical possibilities, but with the progress of the investigation certain regularities became evident and it was possible to eliminate some variants from consideration with reasonable confidence that they would be of higher energy than those investigated.

The preference of Y^{3+} was checked for six species, and in every case except the oxy-amphiboles $M(2)$ was the preferred site. The site preference energies in $(e^2Å^{-1}$ per atom) relative to the next lowest energy isomer involving $M(1)^{3+}$ or $M(3)^{3+}$ were as follows, for the hydroxy-amphiboles:

charge distribution co-ordinates	(022)	(220)	(211)	(112)	(012)	(210)
preference of Y^{3+} for $M(2)$	0.11	0.09	0.09	0.05	0.11	0.006

For the fluoro-amphiboles they were larger by about 0.08, so it follows that covalency in the O-H bond will increase the above preferences, and that even in 210 (pargasite) there will be a substantial preference for Y^{3+} at $M(2)$.

In the oxy-amphiboles the increased negative charge along the central region of the double chain moves the preferred position of Y^{3+} inwards, and $M(1)$ has a preference energy of 0.07 over $M(2)$ and of 0.02 over $M(3)$ (when this is occupied in conjunction with one $M(1)$ site).

The preference of Y^{1+} (or X^{1+}) was checked for six species, and in all hydroxy species $M(4)$ was the preferred site, with preference energies/atom relative to the next lowest energy isomer (involving $M(1)$ or $M(3)$) of:

charge distribution co-ordinates	(022)	(121)	(112)	(012)	(102)	(111)
preferences of Y^+ for $M(4)$	0.14	0.12	0.11	0.13	0.09	0.15

However, in the corresponding fluoro species these preference energies are substantially reduced leaving either a marginal preference energy of the order of 0.01 to 0.05, or even in the case of the species 102 and 121

TABLE 2. CHARGE DISTRIBUTION PATTERNS FOR WHICH MADELUNG ENERGIES
HAVE BEEN COMPUTED. TYPICAL SPECIES CORRESPONDING TO THE CHARGE
DISTRIBUTION CO-ORDINATES ARE GIVEN IN PARENTHESES

202 (tremolite) All M sites M^{2+}; all T sites T^{4+}.

022 (glaucophane) $M(2)^{3+}M(4)^{+}$, $M(2)^{3+}M(1)^{+}$, $M(1)^{3+}M(4)^{+}$, $M(1)^{3+}M(2)^{+}$, $M(2)^{3+}$ $(M(3)^{+}M(4)^{+})$, $M(2)^{3+}(M(1)^{+}M(4)^{+}tr)$.

220 (tschermakite) $M(2)^{3+}T(1)^{3+}$, $M(2)^{3+}T(2)^{3+}$, $M(1)^{3+}T(1)^{3+}$, $M(1)^{3+}T(2)^{3+}$, $M(4)^{3+}$ $T(1)^{3+}$, $M(4)^{3+}T(2)^{3+}$.

211 (common hornblende) $M(3)^{3+}T(1)^{3+}$, $M(3)^{3+}T(2)^{3+}$, $M(1)^{3+}T(1)^{3+}cis$, $M(1)^{3+}T(1)^{3+}tr$, $M(1)^{3+}T(2)^{3+}cis$, $M(1)^{3+}T(2)^{3+}tr$, $M(2)^{3+}T(1)^{3+}cis$, $M(2)^{3+}T(1)^{3+}tr$, $M(2)^{3+}T(2)^{3+}cis$, $M(2)^{3+}T(2)^{3+}tr$.

112 (eckrite) $M(2)^{3+}M(3)^{+}$, $M(2)^{3+}M(4)^{+}cis$, $M(1)^{3+}M(4)^{+}cis$, $M(2)^{3+}M(4)^{+}tr$, $M(3)^{3+}$ $M(1)^{+}$, $M(3)^{3+}M(4)^{+}$, $M(2)^{3+}M(1)^{+}cis$, $M(2)^{3+}M(1)^{+}tr$, $M(1)^{3+}M(3)^{+}$, $M(1)^{3+}$ $M(2)^{+}cis$.

121 (?) $M(2)^{3+}[T(1)^{3+}M(4)^{+}cis]$, $M(2)^{3+}[T(1)^{3+}M(4)^{+}tr]$, $M(2)^{3+}[T(2)^{3+}M(4)^{+}cis]$, $M(2)^{3+}$ $[T(2)^{3+}M(4)^{+}tr]$, $M(2)^{3+}T(2)^{3+}M(3)^{+}$.

102 (richterite) $A^{+}M(4)^{+}$, $A^{+}M(2)^{+}$, $A^{+}M(1)^{+}$, $A^{+}M(3)^{+}$, $A^{2+}M(4)^{+}$.

012 (eckermannite) $A^{+}M(2)^{3+}M(4)^{+}$, $A^{+}M(3)^{3+}M(4)^{+}A^{+}M(1)^{3+}M(4)^{+}$, $A^{+}M(2)^{3+}M(1)^{+}$, $A^{+}(M(2)^{3+}M(4)^{+}cis)M(3)^{+}$, $A^{+}(M(2)^{3+}M(1)^{+}cis)M(3)^{+}$, $A^{+}(M(2)^{3+}M(1)^{+}M(4)^{+}cis)$, $A^{+}(M(2)^{3+}M(1)^{+}cis)M(4)^{+}tr$, $A^{+}(M(2)^{3+}M(4)^{+}cis)M(1)^{+}tr$.

021 (?) $A^{+}M(2)^{3+}M(4)^{+}T(2)^{3+}$, $A^{+}M(2)^{3+}M(4)^{+}T(1)^{3+}$.

120 (mboziite) $A^{+}M(2)^{3+}M(4)^{+}T(1)^{3+}$, $A^{+}M(2)^{3+}M(4)^{+}T(2)^{3+}$.

210 (pargasite) $A^{+}M(3)^{3+}T(1)^{3+}$, $A^{+}M(3)^{3+}T(2)^{3+}$, $A^{+}M(2)^{3+}T(1)^{3+}$, $A^{+}M(2)^{3+}T(2)^{3+}$, $A^{+}M(1)^{3+}T(1)^{3+}$, $A^{+}M(1)^{3+}T(2)^{3+}$.

201 (edenite) $A^{+}T(1)^{3+}$, $A^{+}T(2)^{3+}$.

111 (kataphorite) $A^{+}[M(2)^{3+}M(4)^{+}T(1)^{3+}cis]$, $A^{+}[M(2)^{3+}T(2)^{3+}cis]M(3)^{+}$, $A^{+}[M(2)^{3+}$ $M(4)^{+}T(2)^{3+}cis]$, $A^{+}(M(2)^{3+}M(4)^{+}cis]T(2)^{3+}tr$, $A^{+}[M(2)^{3+}T(2)^{3+}cis]M(4)^{+}tr$, A^{+} $M(2)^{3+}[M(4)^{+}T(2)^{3+}cis]tr$.

The symbols show the sites at which the charges were modified from M^{2+}, T^{4+} and A°. Where two sites of the same type are modified the symbol is not repeated; the occurrence of this can be deduced from the charge distribution co-ordinates on the left, or from the ideal formula of the type species in parenthesis.

In the species 220, 210, and 120 where two T sites are modified, three isomeric possibilities exist for each entry depending on whether the two modified T sites are related to one another by the symmetry plane, the centre of symmetry, or the 2-fold axis. The isomer with the axial symmetry is further split into two isomers in some cases depending on whether the two T sites are *cis* or *trans* to modified M sites. Where such isomeric possibilities occur each was calculated separately.

making $M(3)$ the preferred site by a margin of 0.01 to 0.02. It follows that the reduction of charge on $O(3)$ arising from the covalency in the O-H bond will reduce the preference of Y^{1+} (or X^{1+}) for $M(4)$ but is unlikely to destroy it. No check was made for the oxy-amphiboles but it is evident that the preference for $M(4)$ will be even greater in this case than it is for the hydroxy-amphiboles.

For the 102 (richterite) type of composition the relative energies were calculated for the alternative ionic distributions: X^{+} at A, $X^{2+}X^{+}$ at

$M(4)$; and X^{2+} at A, X_2^{+} at $M(4)$. In hydroxy- and fluoro-forms the preference energies for the first configuration were respectively 0.41 and 0.36 $e^2\text{Å}^{-1}$ on the basis of the cummingtonite structure and 0.28 and 0.20 $e^2\text{Å}^{-1}$ on the basis of the glaucophane structure.

The preference of Z^{3+} was checked for all eight species in which this substitution occurs. Since the different sizes of the $M(2)$ and $M(4)$ sites in glaucophane do not directly affect this preference, it was possible to compare the results obtained using the atomic positions in glaucophane with those from cummingtonite, and so to check whether preference energies are likely to be affected seriously by minor structural differences between different species.

In the three species (220, 211 and 121) in which the A-site is empty, $T(2)$ is the preferred site for Z^{3+}, with preference energies of the order of 0.05, 0.02, and 0.03 respectively when based on the glaucophane structure, and 0.05, 0.07, and 0.02 when based on the cummingtonite structure. These figures were only affected by OH-F substitution to the extent of ± 0.01. In the five species with the A-site filled (*i.e.*, 201, 111, 021, 210, and 120) $T(1)$ is the preferred site for Z^{3+}, with small preference energies 0.04, 0.03, 0.02, 0.02, and 0.02 when based on the glaucophane structure and larger ones of 0.05, 0.07, 0.06, 0.05, and 0.05, when based on the cummingtonite structure. These figures are affected by 0.01 or less as a result of OH-F substitution.

The preferred T sites for Z^{3+} for the various species are shown in Figure 3 on the projected form of the charge distribution plot of the calc-alkali amphiboles (Whittaker, 1968), and are seen to be highly systematic when considered in this way.

In the above discussion of preference energies the figures quoted relate to the lowest energy isomers where $T(1)$ and $T(2)$ substitution can each lead to various positional isomers. When two Z^{3+} ions are present the lowest energy is obtained when these are related to one another by the 2-fold axis in 210 (*e.g.*, paragasite) and in 120 (*e.g.*, mboziite), but when they are related by the mirror plane in 220 (*e.g.*, tschermakite). Where *cis-trans* isomerism is possible the lowest energy is normally attained where the site(s) at which charge is reduced below that in tremolite is (are) cis to the site(s) at which charge is increased. The only exception to this is in the unknown species 121, where the lowest energy configuration has Z^{3+} in $T(2)$ cis to Y^{1+} (or X^{1+}) in $M(4)$. This is presumably due to interchain effects having a dominant influence rather than intra-chain effects.

Total Madelung Energies. The total Madelung energies for the lowest energy isomer calculated from hydroxy-glaucophane, fluoro-glaucophane, hydroxy-cummingtonite, and fluoro-cummingtonite co-ordinates for
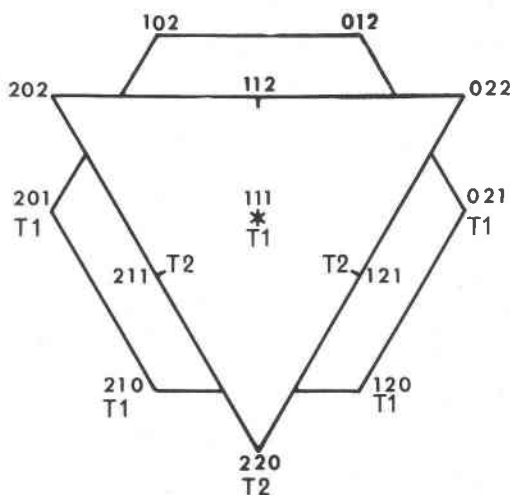
FIG. 3. The projection, perpendicular to its two large faces, of the figure joining the integral points of charge distribution space for the amphiboles (Whittaker, 1968). The co-ordinates of the 13 integral points are shown. For the species which contain tetrahedral $A1$, $T(1)$ or $T(2)$ indicates the site at which such substitution leads to the lowest Madelung energy.

each of the thirteen integral points of amphibole charge distribution space (Whittaker, 1968) are shown in Figures 4 a, b, c, and d respectively. In every case the relative energies are in the same order: that for the 022 amphibole (such as glaucophane) is the lowest; and as one moves anti-clockwise round the triangular face of the diagram (amphiboles with A-site empty) the energy rises progressively through the sequence 112, 202, 211, 220 (eckrite, tremolite, common hornblende, tschermakite) and then falls more rapidly back to the 022 vertex. For the hexagonal face the energy of 012 (eckermannite) is the lowest, although higher than for the 022 vertex; then as one moves round anticlockwise there is an increase as far as 210 (pargasite) followed by a decrease again. The amphiboles 112, 211, 121, and 111, whose compositions can be expressed as equimolar mixtures of vertex compositions, have Madelung energies close to the arithmetic mean of those of the appropriate vertex compositions but differing from them in an unsystematic way. The difference is such that for 111 the single phase is in all cases of lower energy than the mixture, and for 121 always of higher energy. For the other two the difference is sometimes in one direction and sometimes the other and averages very close to zero.

In real calc-alkali amphiboles[1] the $M(4)$ site is always occupied by a large cation, so that in this respect the values of Figures 4c or d are

_____

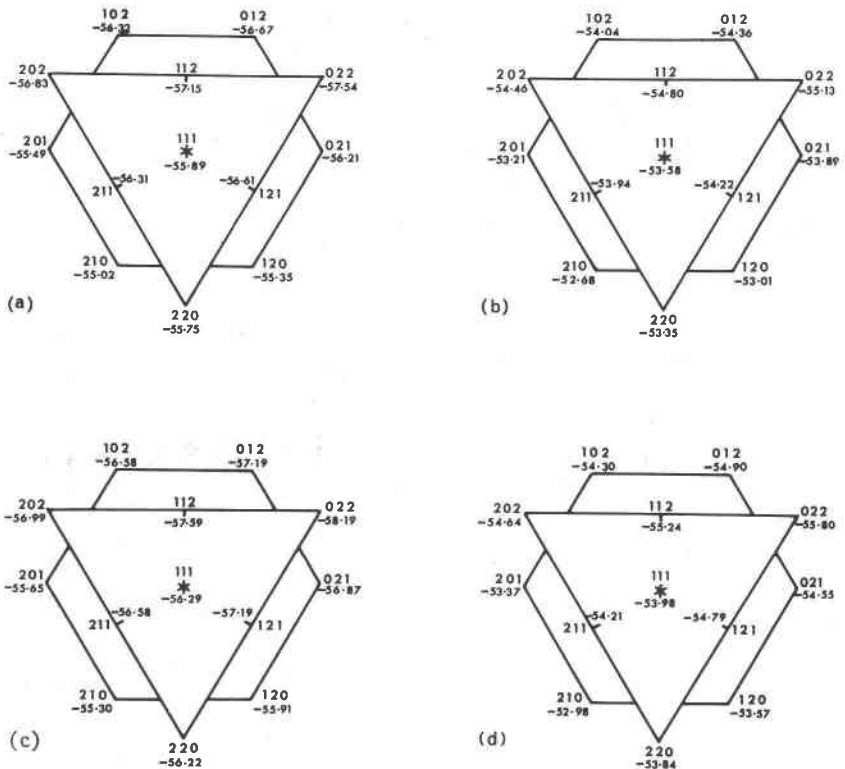[1] This term is taken to exclude clino-holmquistite.

FIG. 4. Total Madelung energies for clino-amphiboles corresponding to the 13 integral points of charge-distribution space: (a) and (b) based on the atomic co-ordinates in the cummingtonite structure, (c) and (d) based on those in the glaucophane structure; (a) and (c) hydroxy-amphiboles, (b) and (d) fluoro-amphiboles.

directly applicable. All the species on the right hand side of the diagram have a small cation (Al^{3+} or Fe^{3+}) at $M(2)$, and the effect of this on the glaucophane-based calculations is therefore approximately correct. The loss of this effect on the left-hand side will actually increase still further the rise of energy above that calculated. Similarly the expansion of T-sites containing Al^{3+} will also increase still farther the rise of energy towards the bottom of the diagram. Thus the species at the top right of the diagrams will be even more relatively preferred than is indicated by the calculated figures.

COMPARISON WITH OBSERVATIONS AND SCALING OF RESULTS

The results obtained are in qualitative agreement with the known cation preferences of Al^{3+} for $M(2)$ in glaucophane (Papike and Clark, 1969), Fe^{3+} for $M(2)$ in magnesioriebeckite and riebeckite (Whittaker,

1949; Burns and Prentice, 1968; Bancroft and Burns, 1969), and Al^{3+} for $T(1)$ in hornblende from Kakanui (charge distribution co-ordinates (1.74, 1.34, 0) near to the pargasite values, but containing appreciable K and Ti) whose structure was determined by Papike, Ross, and Clark (1969). In addition it is tempting to correlate the fact that the amphibole 121 is unknown with the fact that its Madelung energy is always found to be appreciably higher than the mean of 022 (glaucophane) and 220 (tschermakite). The preference of Li^+ for $M(4)$ in holmquistite cannot be correlated directly with the present results, since these do not apply to the ortho-amphibole structure. However it is encouragingly in line with them, and an analysis of the situation in ortho-amphiboles will be presented in a subsequent paper.

Quantitative comparison of the results with observation is more difficult and depends on a number of parameters whose values are imperfectly known. The degree of segregation of ions into particular sites is in general only known approximately. Papike and Clark do not estimate the degree of ordering of $Al^{3+}+Fe^{3+}$ as less than total in glaucophane, and from the $M(2)$-O bond lengths it seems unlikely that less than 90 percent of the trivalent ions in their structure are located at $M(2)$. If one allows for the relative numbers of $M(2)$ and $M(1)$ and $M(3)$ sites this suggests an energy preference of at least 5 Kcal/gm. atom if ordering occurred at 500°K (which is a reasonable value in round figures). Burns and Prentice (1968) give *ir* results that lead to corresponding values of 5–6 kcal for low temperature riebeckites and magnesio-riebeckites, assumed to have ordered at a similar temperature. However, because ordering in riebeckite only involves transfer of an electron and not the interchange of atomic positions there seems to be good reason to suppose that the effective ordering temperature might be about 300°K, in which case the preference energy would be 3–4 kcal. In the case of their pargasite, Papike, Ross and Clark give estimates of the Al^{3+} segregation in $T(1):T(2)$ by three different methods and obtain 0.37:0.13, 0.43:0.07 and 0.34:0.16. The average of these is 0.38:0.12. The ordering temperature here is likely to be higher, in the range 500–1000°K, which corresponds to a preference energy of about 1–2 kcal/gm. atom.[1]

We thus have the following approximate correspondences:

	Obs. preference energy, kcal	*Calc. Madelung preference energy* $e^2\text{Å}^{-1}$
glaucophane	5	0.12
riebeckite	3–5	0.12
pargasite	1–2	0.015

[1] An exact calculation is not possible because of the many possible isomers and the uncertainty as to the size of the domains within which differently oriented forms of the same isomer may be segregated.

A direct calculation gives 1 kcal $= 0.003$ $e^2\text{Å}^{-1}$, so that the calculated Madelung preference energies are of the order of 2.5 to 13 times the observed ones. Such a discrepancy is to be expected for the following reasons. The Madelung energies assume point charges, equal to the oxidation number of the atoms, interacting in a vacuum. Although energies calculated in this way are known to give tolerable agreement with the binding energy of salt-like structures, when allowance is made for ionic repulsions, this agreement arises only because the Madelung energy for the totally ionic structure is reasonably similar to the sum of the ionic and covalent contributions to the binding. In the present work, however, the difference in Madelung energies of two isomeric structures may greatly exaggerate their true difference. The covalent contributions will in practice substitute for part of the ionic binding energy of nearest neighbors, but will also cause the disappearance of a corresponding proportion of the electrostatic energy due to more remote charges. If the true charges on the atoms were uniformly reduced by the electron sharing to a half of the oxidation numbers, the differences in energy between isomers would be reduced by a factor of four. In addition to this the polarizability of the electron clouds around the atoms will further reduce the energy differences by a factor of the order of the square of the refractive index ($\sim$2.6). Thus an overall factor of the order of 10 could readily be accounted for. A following paper will discuss these effects in detail.

Conclusions

It is unlikely that the preference of any particular ion for any particular site will be governed solely by the electrostatic component of the bonding. Specific covalent effects, and geometrical strain due to ionic size differences, will always play some part; and wherever transition metal atoms are involved ligand field effects must also be taken into account where appropriate. Nevertheless the good qualitative and semi-quantitative agreement between the present results and known ionic preferences in glaucophane, riebeckite, pargasite, and (less directly) holmquistite shows that such electrostatic effects may well often have a dominant influence. If this dominance is maintained then the following predictions are possible:

(i) richterite Na_2Ca Mg_5 $Si_8O_{22}(OH)_2$ should have Na at A and Ca, Na at $M(4)$, not Ca at A and Na_2 at $M(4)$[1].

[1] This prediction is in line with the generally accepted assumption, but it has never been proved. In the richterite studied by Papike, Ross and Clark (1959). K,Na,Ca was present and K was shown to occupy the A site. This would be necessitated by the size of K, and it does not follow that Na would do the same. The rarity of eckrite Na $CaMg_4Al$

(ii) clino-holmquistite should have Li_2 at $M(4)$.

(iii) fluoro-lithio-magnesio-richterite LiNa Mg_6 $Si_8O_{22}F_2$ should have Na at A, Mg_2 at $M(4)$ and Li at $M(3)$.

(iv) oxy-amphiboles should have a preference for Y^{3+} or Y^{4+} at $M(1)$. This should apply to Fe^{3+} in oxidised grunerite $Fe_5^{2+}Fe_2^{3+}$ $Si_8O_{22}O_2^{2-}$ and perhaps to Ti^{4+} in kaersutite $NaCa_2$ Mg_3FeTi $Si_6Al_2O_{23}OH$.

(v) $M(2)$ should be the preferred site for Y^{3+} in all other cases that have not been examined in this connection (*i.e.*, all amphiboles containing Y^{3+}, other than oxy-amphiboles).

(vi) $T(2)$ should be preferentially occupied by Al in common hornblende Ca_2 Mg_4Al $Si_7AlO_{22}(OH)_2$ and tschermakite Ca_2 Mg_3Al_2 Si_7Al $O_{22}(OH)_2$.

(vii) $T(1)$ should be preferentially occupied by $A(l)$ in edenite $NaCa_2$ $(Mg,Fe)_5$ Si_7Al $O_{22}(OH)_5$, kataphorite Na_2Ca $(Mg,Fe)_4(Al,Fe)$ $Si_7AlO_{22}(OH)_2$, and mboziite Na_2Ca $(Mg,Fe)_3(Al,Fe)_2$ $Si_6Al_2O_{22}$ $(OH)_2$.

References

BANCROFT, G. M., AND BURNS, R. G. (1969) Mössbauer and absorption spectral study of alkali amphiboles. *Mineral. Soc. Amer. Spec. Pap.* **2**, 137–148.

BOEYENS, J. C. A., AND GAFNER, G. (1969) Direct summation of Madelung energies. *Acta. Crystallogr.* **A25**, 411–414.

BURNS, R. G., AND PRENTICE, F. J. (1968) Distribution of iron cations in the crocidolite structure. *Amer. Mineral.* **53**, 770–776.

DONNAY, G., AND ALLMAN, R. (1970) How to recognise O^{2-}, OH^- and H_2O in crystal structures determined by X-rays. *Amer. Mineral.* **55**, 1003–1015.

EVJEN, H. M. (1931) On the stability of certain heteropolar crystals. *Phys. Rev.* **39**, 675–687.

GAIT, R. I., AND FERGUSON, R. B. (1970) Electrostatic charge distributions in the structure of low albite, Na Al Si_3O_8. *Acta. Crystallogr.* **B26**, 68–77.

GHOSE, S. (1961) The crystal structure of a cummingtonite. *Acta. Crystallogr.* **14**, 622–627.

JAGODZINSKI, H. (1967) Some new aspects of the solution of disorder problems. *Bull. Soc. Franc. Mineral Cristallogr.* **90**, 575–584.

PAPIKE, J. J., AND CLARK, J. R. (1968) The crystal structure and cation distribution of glaucophane. *Amer. Mineral.* **53**, 1156–1173.

$Si_8O_{22}(OH)_2$ and the fact that 121 (NaCa Mg_3Al_2 $Si_7AlO_{22}(OH)_2$) is not known could be taken to suggest that the sharing of $M(4)$ sites by NaCa is unstable, and that richterite would prefer Ca at A. The present work negatives this possibility.

PAPIKE, J. J., ROSS, M., AND CLARK, J. R. (1969) Crystal chemical characterization of clino-amphiboles based on five new structure refinements. *Mineral. Soc. Amer. Spec. Pap.* **2,** 117–136.

WHITTAKER, E. J. W. (1949) The structure of Bolivian crocidolite. *Acta. Crystallogr.* **2,** 312–317.

———, (1968) Classification of the amphiboles. *In* International Mineralogical Association, *Proceedings of the 5th General Meeting,* 1966. Mineralogical Society, London, 232–242.

——— (1969) The structure of the orthorhombic amphibole holmquistite. *Acta Crystallogr.* **32,** 394–397.

ZUSSMAN, J. (1955) The crystal structure of an actinolite. *Acta Crystallogr.* **8,** 301–308.